Theory of the de Haas–van Alphen effect during magnetic breakthrough of conduction electrons with a spin-orbit interaction

Yu. N. Proshin and N. Kh. Useinov

Kazaan' State University, 420008 Kazan', Russia
(Submitted 11 December 1992; resubmitted 5 October 1993)
Zh. Eksp. Teor. Fiz. **105**, 139–155 (January 1994)

A theory of magnetic breakdown (MB), in which the spin of the conduction electron is flipped, has been developed. The general expressions for the oscillating parts of the number density of states and for the thermodynamic potential have been derived in the form of multiple Fourier series under the conditions of magnetic breakdown, with allowance for the spin–orbit coupling. The coefficients of these series are expressed in terms of the product of the elements of a full MB s-matrix of fourth rank. The amplitude characteristics of the de Haas–van Alphen effect for the main orbits in zinc are found to change considerably when the spin degrees of freedom are taken into account. For this metal the theory which is being developed is found to be in qualitative agreement with the known experimental data on the oscillation of the de Haas–van Alphen effect on a "needle."

Oscillations of the thermodynamic potential and its derivatives in a magnetic field—the de Haas–van Alphen effect—provide reliable information on the energy structure of metals and on their Fermi surfaces.[1] These oscillations arise as the Fermi energy $\mathscr{E}_F$ is crossed by a succession of quasiequidistant discrete energy levels as the strength of the magnetic field is varied. Here there must be closed electron trajectories on the Fermi surface which satisfy the following equations in the semiclassical approximation:[2]

$$\mathscr{E}_{n\sigma}(\mathbf{p})=\mathscr{E}_F=\text{const}, \quad p_z=p_{z0}=\text{const}, \tag{1}$$

where $\mathscr{E}_F$ is the Fermi energy, $\mathbf{p}$ is the quasimomentum, p_z is the projection of the quasimomentum onto the magnetic field $\mathbf{H}$, n specifies the band, and $\sigma=\uparrow,\downarrow$ is the spin index.

A topological restructuring of electron trajectories occurs in certain metals in sufficiently strong magnetic fields, and so-called magnetic breakthrough occurs. This term represents a set of phenomena which stem from the tunneling of a conduction electron between semiclassical trajectories of different bands separated by an anomalously small energy gap.

The theory of magnetic breakthrough has been developed extensively. It is presented in detail in reviews by Stark and Falikov[3] and Kaganov and Slutskin.[4] The theory for the de Haas–van Alphen effect is presented in detail in the book by Shenberg.[1] That book also presents the theory of magnetic breakthrough and cites a long list of theoretical and experimental studies of these questions. It follows from these papers that small regions in which two bands come anomalously close to each other (and in which the semiclassical approximation[2]—the customary approximation for metals—is not valid) can be thought of as centers of a quantum interband scattering of electrons in quasimomentum space and can be called "magnetic breakthrough sites."[4] Under magnetic breakthrough conditions, the topology of the trajectories of conduction electrons in (1) changes: in quasimomentum space, a plane network of semiclassical regions belonging to different bands and linked by magnetic breakthrough sites forms. This network is called a "magnetic breakthrough configuration."[1)] The motion of conduction electrons along a magnetic breakthrough configuration is a probabilistic process, and the wave functions of different regions are related to each other by s-matrices. These matrices describe a two-channel magnetic-breakthrough scattering of conduction electrons by magnetic-breakthrough sites. These matrices do not incorporate a spin–orbit interaction. The energy spectrum (the "magnetic-breakthrough spectrum") which arises in the course of magnetic breakthrough occupies an intermediate position between a strictly deterministic spectrum under semiclassical conditions and a completely stochastic spectrum of disordered systems.

There are various ways to calculate the oscillatory increments in thermodynamic properties in the case of magnetic breakthrough. The method of Falikov and Stakhovyak[5] is based on a theorem which relates the density of states to the Fourier transformation of a Green's function. This function corresponds to a superposition of semiclassical wave packets which return to a given point in the magnetic-breakthrough network of bound orbits along all possible paths. Their amplitudes decrease in the process in accordance with the number of magnetic-breakthrough sites which they pass, while their phases are determined by the areas of the sectors traced out by these trajectories. Another method, proposed by Slutskin,[4] is to represent the oscillatory part of the number density of states, $\tilde{\nu}(E,p_z)$, as the sum of multiple Fourier series. The coefficients of this series can be expressed in terms of a product of the elements of the s-matrices of the given magnetic-breakthrough configuration. The phases are proportional to the areas of the closed orbits constructed from the semiclassical regions.

However, these papers[1,3–5] discussed effects associated with only the orbital motion of the conduction electrons during magnetic breakthrough; there was essentially no discussion of the spin properties of the conduction electrons. It was shown in Ref. 6 that incorporating the spin–

 1063-7761/94/010073-10$10.00

orbit interaction and the spin degrees of freedom of the conduction electrons into the theory of magnetic breakthrough leads to a substantial change in a basic dynamic characteristic of the magnetic-breakthrough s-matrix. When the spin of the conduction electrons is taken into account, this matrix becomes a 4×4 matrix, while the spin–orbit interaction gives rise to a probability for breakthrough with spin flip. Incorporating the spin–orbit interaction thus renders the magnetic-breakthrough scattering a three-channel process; that circumstance in turn leads to a significant complication of the magnetic-breakthrough spectrum.[7] A systematic theory of magnetic breakthrough incorporating the spin of the conduction electrons and the spin–orbit interaction in the relaxation-time approximation[8] yields a very good explanation of the experimentally observed[9] doubling of the peaks of the magnetic-breakthrough oscillations of the galvanomagnetic characteristics of zinc.

In this situation it is obviously worthwhile to take a theoretical look at the effect of the spin–orbit interaction on oscillations in the density of states under the conditions of coherent magnetic breakthrough, since a spin flip of the conduction electrons in the course of magnetic breakthrough leads to an interference of semiclassical states of conduction electrons with different spin directions. This interference should undoubtedly be reflected in the de Haas–van Alphen effect.[6]

In the present paper we derive an expression for the oscillatory part of the thermodynamic potential under magnetic-breakthrough conditions, incorporating the spin–orbit interaction (Sec. 2). In Sec. 3 we calculate the amplitudes for the de Haas–van Alphen effect and the main orbits of the 2D magnetic-breakthrough network which arises in Zn when the magnetic field is directed along the hexagonal axis. The band gap in zinc is of a spin–orbit nature.[1,3,10] The probability for magnetic breakthrough with spin flip becomes substantial in this case,[6] making it necessary to use the theory which we have derived for this metal. In Sec. 4 we derive an expression for the second derivative of the magnetization with respect to the field. This expression describes the de Haas–van Alphen effect at "needles" in Zn under magnetic-breakthrough conditions. We compare a plot of this field dependence with the experimental curve from Ref. 10. The theoretical curve is plotted with parameter values from Ref. 8, which were extracted from experimental data on the galvanomagnetic properties of Zn under magnetic-breakthrough conditions.[9] In the following section of the paper we take a brief look at the coherent motion of conduction electrons along a magnetic-breakthrough configuration with spin flip at magnetic-breakthrough sites. It then becomes possible to express the oscillatory part of the density of states in terms of the magnetic-breakthrough spectrum.

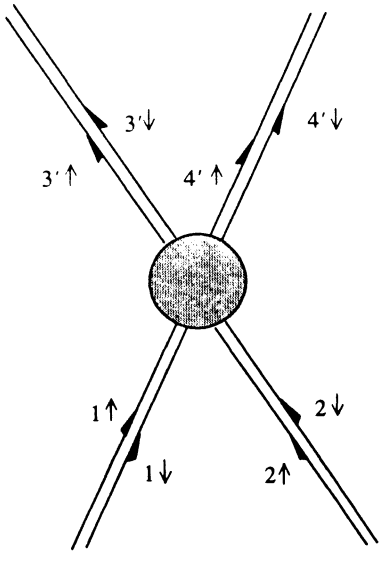

FIG. 1. Depiction of magnetic breakthrough vertex (1 and 2 are incoming segments of the quasiclassical trajectories, 3′ and 4′ are outgoing). Arrows indicate the direction of conduction electron motion and the direction of the spin σ.

1. COHERENT MAGNETIC BREAKTHROUGH WITH SPIN FLIP

We consider the coherent motion of conduction electrons or the time evolution of a semiclassical wave packet along a magnetic-breakthrough configuration, taking spin degrees of freedom into account.

The motion of the conduction electrons is coherent under the conditions[4] τ, $\tau_{sa}\gg1/\omega_c$, where τ is the relaxation time, τ_{sa} is the small-angle scattering time, and ω_c is the cyclotron frequency. In taking the spin degrees of freedom into account below, we assume everywhere that the typical spin relaxation time τ_s is much longer than any other time scale of the problem (τ, τ_{sa}, or ω_c^{-1}). This condition is valid for pure metals and low temperatures. The spin flip of conduction electrons in the course of motion along a magnetic-breakthrough configuration is thus governed by magnetic-breakthrough scattering alone. In this case, each semiclassical region of trajectory (1) can be characterized by the set $i\sigma$, where i specifies the region, and σ specifies the spin direction of the conduction electron in this region. The band index n is uniquely determined by the region index i. We denote by $|t;i\sigma\rangle$ a wave packet—a state with a finite momentum uncertainty ΔP and a finite coordinate uncertainty ΔR—which is localized in region i at time t. As it moves along the semiclassical region $i\sigma$ to the nearest magnetic-breakthrough site, the wave packet acquires a phase shift

$$\varphi_{i\sigma}(E,P_z)=\varphi_i/\hbar+\delta_i+\gamma^s_{i\sigma}, \tag{2}$$

where $\varphi_i(E,p_z)$ is the increment in the transverse action, $\delta_i=\pm\pi/2$ is the sum of all phase shifts which occur in region i during passage through classical turning points, and

$$\gamma^s_{i\sigma}(E,p_z)=\pm\frac{1}{2}\pi\frac{m_{i\sigma}}{m_0}g_i \tag{3}$$

is the spin contribution to the phase shift, which stems from the Zeeman splitting of the spin energy levels in the

magnetic field when spin–orbit interaction is taken into account.[6,11] In (3), the quantities $g_i=g_i(E,p_z)$ and $m_{i\sigma}=m_{i\sigma}(E,p_z)$ are the g-factor and effective cyclotron mass of a conduction electron in region i, m_0 is the mass of a free electron, the plus sign corresponds to $\sigma=\uparrow$, and the minus sign to $\sigma=\downarrow$.

Each magnetic-breakthrough site (a schematic diagram of which is shown in Fig. 1) is a center of quantum-mechanical scattering of electrons, which is connected to eight semiclassical regions when spin is taken into account. After passing through magnetic-breakthrough sites, a semiclassical packet $|t;i\sigma\rangle$ splits into three parts in accordance with the expression

$$|t;i\sigma\rangle=\sum_{i'\sigma'} s_{i\sigma,i'\sigma'}|t;i'\sigma'\rangle, \tag{4}$$

where the primes specify the regions (and the corresponding spin projections) which emerge from the magnetic-breakthrough site (Fig. 1). The scattering amplitudes in (4) are elements of an s-matrix, which can be written as follows when the spin–orbit interaction is taken into account:[6]

$$\hat{s}=\begin{bmatrix} \tau\exp(\mp i\Lambda) & 0 & \pm\rho/\beta & \pm\alpha\rho/\beta \\ 0 & \tau\exp(\mp i\Lambda) & \mp\alpha\rho/\beta & \pm\rho/\beta \\ \mp\rho/\beta & \pm\alpha\rho/\beta & \tau\exp(\pm i\Lambda) & 0 \\ \mp\alpha\rho/\beta & \mp\rho/\beta & 0 & \tau\exp(\pm i\Lambda) \end{bmatrix}, \tag{5}$$

$$\rho^2=\exp(-H_0/H)=w, \quad \tau^2+\rho^2=1, \quad \beta=(1+\alpha^2)^{1/2}, \tag{5a}$$

where w is the total probability for an interband transition of a conduction electron, H_0 is a characteristic breakdown field, which incorporates the spin–orbit interaction, and α is a parameter of the spin–orbit interaction in magnetic-breakthrough theory. The s-matrix parameters (H_0 and α) depend on the characteristics of the band spectrum of the metal and on the matrix element of the velocity operator of the conduction electron, calculated at the center of the magnetic-breakthrough site ($\mathbf{p}=\mathbf{p}_M$). Exact expressions for these parameters are given in Ref. 6; here we will simply mention that an estimate of α shows that α is on the order of one when the spin–orbit interaction has a strong effect, while $0\leqslant a\ll 1$ when the spin–orbit interaction is weak. We would also point out that if the spin–orbit interaction is ignored ($\alpha=0$, $\beta=1$) then all results reduce to those derived previously in magnetic-breakthrough theory.[3,4] The choice of signs in (5) is determined by the sign of the difference

$$[\mathscr{E}_{n\sigma}(\mathbf{p}_M)-\mathscr{E}_{n'\sigma'}(\mathbf{p}_M)], \quad n=n(i) \text{ and } n'=n'(i'). \tag{5b}$$

The upper signs correspond to the positive value in (5b).

The quantities ρ, τ, and Λ in (5) are real functions of $\mathbf{H}$, H_0, $\mathscr{E}_F$, and p_z. The quantity Λ can be written as a function of H_0/H as follows:

$$\Lambda=\frac{\pi}{4}+\frac{H_0}{\pi H}+\arg\Gamma\left(i\frac{H_0}{\pi H}\right)-\frac{H_0}{\pi H}\ln\frac{H_0}{\pi H}. \tag{5c}$$

This expression determines the phase shift of the wave function of a conduction electron in the course of magnetic breakthrough; $\Gamma(x)$ is the gamma function.

To streamline the equations, we replace the two symbols $i\sigma$ by the one symbol i for a semiclassical region. Odd-numbered regions correspond to states of the conduction electron with spin up, and even-numbered regions to states with spin down: $\sigma=\uparrow$ and $\sigma=\downarrow$, respectively. The new region label i uniquely determines the index of the band and the spin direction of the conduction electron: $n\sigma=n\sigma(i)$.

Incorporating the spin degrees of freedom and the existence of a third scattering channel ($\alpha\neq 0$) doubles the number of semiclassical regions of trajectory (1) making up the magnetic breakthrough configuration (in comparison with that in Refs. 1 and 3–5). The number of nonequivalent regions also doubles. In this sense, the results of this section of the paper constitute a simple generalization of the results presented in a review.[4] Here it is necessary to assign various numbers ($i,j,\ldots$) from 1 to N to nonequivalent regions. In the case of a closed magnetic breakthrough configuration, the total number of regions serves as N.

The wave packet $|t;i'\rangle$ which arises after magnetic breakthrough scattering evolves in a semiclassical fashion until it is scattered by the next magnetic breakthrough site, etc. The scattering occurs at the times

$$t_{\mathbf{L}}=\sum_{i=1}^{N} l_i T_i\equiv\mathbf{LT}, \tag{6}$$

where T_i is the time of motion through region i, and the nonnegative integers l_i represent the number of passages of a conduction electron through region i. The time $t_{\mathbf{L}}$ is reckoned from the time of the first scattering.

In expression (6) we have introduced the N-dimensional vectors $\mathbf{L}(l_1,\ldots l_N)$ and $\mathbf{T}(T_1,\ldots T_N)$.

As a result of multiple scattering, the semiclassical packets proliferate exponentially in time. In the case of closed magnetic breakthrough configurations, these packets interfere, forming a packet with a resultant amplitude

$$A_{i,j}(\mathbf{L})=A_{i,j}(l_1,l_2,...l_i,...l_j,...l_N),$$

$$i=1,2,...N, \quad j=1,2,...N. \tag{7}$$

When spin and the spin–orbit interaction are ignored, this amplitude satisfies the recurrence relations derived by Slutskin.[12]

The mathematical tools developed in Ref. 13 for analyzing magnetic breakthrough configurations and for constructing corresponding dispersion relations under magnetic breakthrough conditions do not impose any limitations on the form or rank of the s-matrices. On this basis we make use of the results of Ref. 13, and we also write a few formulas which make it possible to express the oscillatory part of the density of states, $\nu(E,p_z)$, as multiple Fourier series of semiclassical phase shifts and resultant amplitudes $A(\mathbf{L})$:

$$\tilde{\nu}(E,p_z)=\frac{1}{\pi\hbar}\sum_{i}^{N} T_i \sum_{\mathbf{L}}{}' \bar{A}_{i,i}(\mathbf{L})\cos(\mathbf{L}\gamma). \tag{8}$$

The quantity $\bar{A}_{i,j}(\mathbf{L})$ is the smooth part of the amplitude, consisting of a product of corresponding elements of s-matrices corresponding to magnetic breakthrough sites through which path $\mathbf{L}$ passes. The quantities $\bar{A}_{i,j}(\mathbf{L})$ are the quantum probability amplitudes for finding a conduction electron in region j at a time $\mathbf{LT}$ after the first scattering by the starting region i. To generate a complete description of the dynamics of the conduction electrons under magnetic breakthrough conditions, we need to know the entire infinite set of amplitudes $\bar{A}_{i,j}(\mathbf{L})$. In expression (8) it is not possible to carry out the summation over the spin σ explicitly, in contrast with the situation in equation (4.2.3) of Ref. 4. The reason is our incorporation of the spin–orbit interaction.

In the sum over $\mathbf{L}$ in (8), the only nonvanishing amplitudes $\bar{A}_{i,j}(\mathbf{L})$ are those with $\mathbf{L}$'s which generate closed trajectories which pass through region i. All closed trajectories which begin and end in region i generate all possible closed j-paths. Each j-path passes l_k times through the kth region of the closed trajectory ($k=1,2,...,N$). For a given $\mathbf{L}$, the j-paths differ from each other in the order of passage through semiclassical regions of the magnetic breakthrough network. Corresponding to the order of the passage of a j-path is a certain sequence of region labels $[i,...,i]$. The first and last terms of this sequence are the same as the first and second subscripts in $\bar{A}_{i,j}(\mathbf{L})$. Writing the given $\mathbf{L}$'s in the form $\mathbf{L}=r\mathbf{j}$, we have the following equation for the amplitude $\bar{A}_{i,j}(\mathbf{L})$:

$$\bar{A}_{i,i}(\mathbf{L})=j_i R_b(r\mathbf{j}), \tag{9}$$

where $\mathbf{j}$ is an N-vector with mutually simple integer components which have no common divisors, r determines the number of "circuits" of the j-path, and the quantity $R_b(r\mathbf{j})$, which is independent of the index of region i, is uniquely determined by the N-vector $\mathbf{L}=r\mathbf{j}$. Equation (9) shows that the same amplitude $\bar{A}_{i,i}(\mathbf{L})$ corresponds to closed j-paths $[i,...,i',...,i]$ which differ by a cyclic permutation of the terms of the sequence $[i',...,i,...,i']$. Since there exist sequences $[i,...,i]$ which do not change upon cyclic permutation ($i'=i$), the quantity $R_b(r\mathbf{j})$ is identical for all such permutations, and the number of such sequences, j_i, appears in (22).

Accordingly, the sum

$$\sum_{l_1,l_2,...l_N\geqslant 0}{}' \bar{A}_{i,i}(l_1,l_2,...l_N),$$

with $\mathbf{L}$'s which generate closed trajectories, can be written as another sum over j-paths. Working from (8), and using (9), we find

$$\tilde{\nu}(E,p_z)=\frac{1}{\pi\hbar}\sum_{j}\mathbf{T}\mathbf{j}\sum_{r=i}^{\infty}R_b(r\mathbf{j})\cos(r\mathbf{j}\gamma), \tag{10}$$

where the scalar products $\mathbf{T}\mathbf{j}=T_{\mathbf{j}}$ and $\mathbf{j}\gamma=\gamma_{\mathbf{j}}$ give us, respectively, the cyclotron period and the semiclassical phase shift acquired by a conduction electron on the closed trajectory. A conduction electron begins its motion with one spin direction, and after a time $T_{\mathbf{j}}$ it returns to the same point, with the same spin direction.

The summation in (10) is carried out over all possible j's which generate closed j-paths. Following Ref. 4, we call all the j-paths corresponding to the N-vector $\mathbf{j}$ a "j-orbit." The vector $\mathbf{j}$ in (10) embodies information on the spin directions of the conduction electrons in all regions of possible closed orbits.

2. OSCILLATORY PART OF THE THERMODYNAMIC POTENTIAL UNDER MAGNETIC BREAKTHROUGH CONDITIONS WITH A SPIN–ORBIT INTERACTION

In the absence of magnetic breakthrough, quantum oscillations on plots of thermodynamic properties versus the magnetic field can be expressed in terms of the oscillatory part of the density of states, $\tilde{\nu}(E,p_z)$, with given values of E and p_z, as is well known.

A calculation of the oscillatory part of the thermodynamic potential, $\tilde{\Omega}$, with the help of the density of states in (10) can be carried out in the standard way. We will not repeat that well-known, laborious procedure (see, for example, Refs. 1 and 2). We proceed immediately to the final expression for $\tilde{\Omega}$ per unit volume of a metal, but in this expression it is not possible in general to explicitly carry out the summation over spin projections, and the spin index itself is "hidden" in $\mathbf{j}$:

$$\tilde{\Omega}=\left(\frac{e}{2\pi c\hbar}\right)^{3/2}\frac{e\hbar}{2\pi^2 c}H^{5/2}\sum_{\mathbf{j}\xi}\left|\frac{\partial^2 S_{\mathbf{j}}}{\partial p_z^2}\right|^{-1/2}\frac{1}{m_{\mathbf{j}}}$$

$$\times\sum_{r=1}^{\infty}\frac{1}{r^{5/2}}R_T R_b(r\mathbf{j})$$

$$\times\cos\left[r\left(\frac{cS_{\mathbf{j}}^{\xi}(E,p_z)}{e\hbar H}+\gamma_{\mathbf{j}}^{s}+\Lambda_{\mathbf{j}}-2\pi\gamma\right)\pm\frac{\pi}{4}\right]. \tag{11}$$

Here $S_j^{\xi}(E,p_z)$ is the "spinless" area of the closed j-orbit, $2\pi\gamma$ is a constant phase shift, independent of magnetic breakthrough,[2)] and R_T is a thermal factor, given by

$$R_T=\frac{2\pi^2 r k_B T c m_{\mathbf{j}}/\hbar eH}{\mathrm{sh}(2\pi^2 r k_B T c m_{\mathbf{j}}/\hbar eH)}. \tag{12}$$

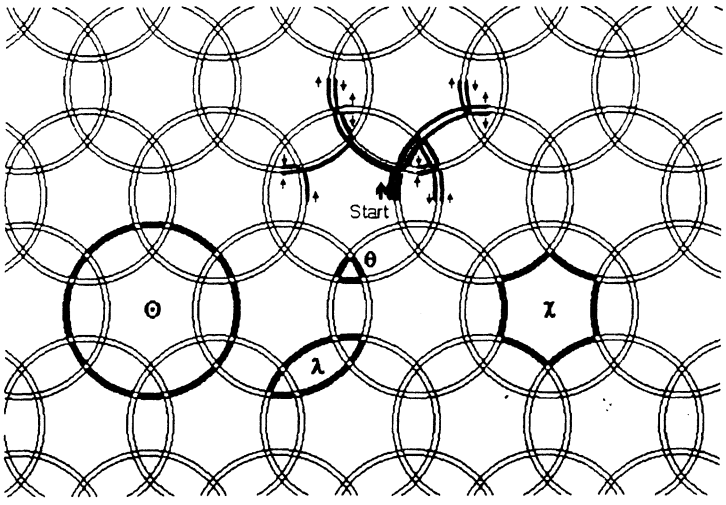

FIG. 2. Depiction of a cross section of the Fermi surface of Zn in the plane $p_z=0$ (the z axis is parallel to the hexagonal axis. Under magnetic breakthrough conditions, a breakthrough lattice is formed with small triangular orbits θ, giant circular orbits $\odot$, dihedral orbits λ, and hexahedral orbits χ (bold). For clarity, triangular orbits have intentionally been magnified. Using the labeled segments, we have also shown several stages in the proliferation of a single quasiclasical wave packet moving through the magnetic breakthrough configuration when conduction electron spin is taken into account. The thickness of the curves roughly corresponds to the breakthrough amplitude of the packets. Arrows indicate spin direction on the initial ("Start") and final segments.

All quantities in (11) and (12) which depend on E and p_z are evaluated at $E=\mathscr{E}_F$ and $p_z=p_z^{\xi}$, where the label ξ specifies the extremal areas of the j-orbits. We also note that in our case, as in Ref. 12, for closed trajectories which do not lie within the first Brillouin zone, all quantities having an index **j** are composite magnetic breakthrough analogs of corresponding semiclassical quantities. In particular, $\gamma_{\mathbf{j}}^{s}$ and $\Lambda_{\mathbf{j}}$ are determined by corresponding sums of the spin contribution in (3) and of the phase shifts of the wave function of a conduction electron upon magnetic breakthrough [see (5c)] along a j-orbit.

For j orbits which lie in a common band and on which the spin of the conduction electron does not flip even in the case $\alpha\neq 0$, it is possible to carry out the summation over spin projections in (11), as in the case of (for example) triangular orbits on "needles" in Zn. The expression for $\tilde{\Omega}$ then acquires a standard spin factor $R_s(j)=\cos(r\pi g_j^s)$, where $g_j^s=(m_j/2m_0)g_j$, is called the "spin splitting parameter of the j-orbit."[3] For such orbits, expression (11) is the same as the expression for $\tilde{\Omega}$ given in Ref. 4, aside from the changes in notation. In the absence of spin–orbit interaction ($\alpha=0$), but with spin states being taken into account, we naturally find a corresponding result.

Expression (11) thus generalizes Slutskin's result[4] to the case in which the spin–orbit interaction must be taken into account under magnetic breakthrough conditions. When the spin degrees of freedom are taken into account, an interference of semiclassical states of conduction electrons with different spin directions in the course of coherent magnetic breakthrough can substantially change the amplitudes of the oscillations in thermodynamic properties.

To conclude this section of the paper, we note that expression (11) ignores dissipative processes in the electron system. The decrease in oscillation amplitude due to the scattering of conduction electrons is taken into account through the introduction of a Dingle factor. As was shown in Ref. 13, the incorporation of a Dingle factor under magnetic breakthrough conditions gives rise to an additional factor R in expression (11) (see also Sec. 4).

3. AMPLITUDES OF THE DE HAAS–VAN ALPHEN EFFECT IN ZINC FOR THE BASIC ORBITS

Let us use the theory derived above to calculate absolute values of the amplitudes for the de Haas–van Alphen effect from four basic orbits which arise in a hexagonal magnetic breakthrough network in Zn (Fig. 2). In expression (11), for r of order unity, the magnetic breakthrough factor $R_b(r\mathbf{j})$ can be calculated in a combinatorial fashion as a sum over j-orbits. A method of this sort was proposed in Ref. 5 for calculating $R_b(r\mathbf{j})$ without consideration of the spin–orbit interaction, as we have already mentioned. A simple illustration of this method is given in Ref. 1 for several important orbits which arise in the course of magnetic breakthrough in Mg. At large values of r, a combinatorial calculation of $R_b(r\mathbf{j})$ becomes very complicated, even if the spin–orbit interaction is ignored. In this case it is more convenient to use an integral representation for $R_b(r\mathbf{j})$ (Ref. 4).

For our main problem—calculating the effect of the spin–orbit interaction on the amplitude for the de Haas–van Alphen effect under magnetic breakthrough conditions—we can use a more graphic combinatorial method with $r=1$. It thus becomes possible to find the magnetic breakthrough factor $R_b(r\mathbf{j})$ in a comparatively simple way and to carry out the summation over spin in (11).

Working from (11) for the main harmonic, $r=1$, and ignoring the Dingle factor, we find the following expression for the susceptibility $d\tilde{M}/dH$ of the jth orbit[4]:

$$\frac{d\tilde{M}_j}{dH}=\left(\frac{e}{c\hbar}\right)^{3/2}\left(\frac{m_0}{m_j}\right)^{1/2}\frac{k_BTF_j^2}{H^{5/2}\,\mathrm{sh}(\alpha T/H)}\sum_{\sigma}R_b(\mathbf{j})$$
$$\times\cos\left(\frac{2\pi F_j}{H}+\gamma_{\mathbf{j}}^{s}+\varphi\right), \qquad (13)$$

where $F_j=cS_j^{\xi}(E,p_z)/2\pi e\hbar$ is the frequency of the de Haas–van Alphen oscillations,[1]

$$a=2\pi^2k_Bcm_j/\hbar e=1.47(m_j/m_0)10^5\ \mathrm{G/K}, \qquad (14)$$

and φ is a constant phase shift which is unimportant here. The mass ratio (m_0/m_j) in (13) follows from the factor $|\partial^2 S_j/\partial p_z^2|$ in expression (11) for circular orbits and for orbits formed from circular arcs (see, for example, p. 413 in Ref. 1 for Mg), as in Zn. In deriving (13) we ignored the spin difference[5] in all composite magnetic breakthrough quantities except the spin contribution to the phase, $\gamma_{\mathbf{j}}^s$, and the magnetic breakthrough factor $R_b(\mathbf{j})$, which determines the amplitude $\tilde{\Omega}$. We also omitted the vector notation for the index j; i.e., we replaced these quantities by corresponding semiclassical quantities.

The scalar symbol j in (13) refers to a set of j-orbits of a common type which envelop a common "spinless" area but which differ in spin direction (i.e., in the sign of $\gamma_{\mathbf{j}}^s$) in at least one of the regions. Within these sets, we need to carry out a partial summation over $\mathbf{j}$; such a summation is essentially an average over the spin.

Since a semiclassical packet splits into three parts as it passes through magnetic breakthrough sites [see (4)], the quantity $R_b(r\mathbf{j})$ for a closed j-orbit is given by the following formula according to the structure of the s-matrix in (5), in which we must set $\Lambda=0$ (Refs. 4 and 13):

$$R_b(r\mathbf{j})=(\pm\rho/\beta)^{n_{1j}}(\tau)^{n_{2j}}(\pm\alpha\rho/\beta)^{n_{3j}}, \tag{15}$$

where n_{1j} is the number of breakthroughs without spin flip, n_{2j} is the number of reflections, n_{3j} is the number of breakdowns with spin flip on the j-orbit, and the sign for each magnetic breakthrough site is determined in accordance with the discussion of expressions (5) and (5b). We assume for simplicity that all magnetic breakthrough sites are equivalent.

The identical magnetic breakthrough factors in (15) and the different signs of $\gamma_{\mathbf{j}}^s$ in phase (13) give us, after an averaging over the spin, the factor $R_s(j)=\cos(\pi g_j^s)$ from any pair of j-orbits which are of a common type. The field dependence of the amplitude $d\tilde{M}_j/dH$ of the jth orbit is determined by the sum over all orbits which belong to a common type, with the difference in spin directions being taken into account. Each term of the sum must be multiplied by a corresponding magnetic breakthrough factor (15) and by a factor $R_s(j)$, which arises after the average is taken over the spin. In addition, another weight factor C_j will correspond to some of the paths. This factor arises from the symmetry and is equal to the number of ways in which orbit j can be constructed.[1,5]

We now consider the hexagonal magnetic breakthrough network of Zn, allowing for the doubling of the number of regions due to spin–orbit interaction (Fig. 2). From this network we single out four main orbits (Fig. 3): a gigantic circular orbit $\odot$, which arises because of the magnetic breakthrough; a triangular orbit θ, from the "needles"; a lune-shaped orbit λ, which combines large regions from a "monster" with small regions from needles; and a hexagonal orbit χ from the monster, whose area is negative. In this manner we incorporate a traversal of this hole orbit by a conduction electron in the direction opposite the rotation along electron orbits $\odot$, θ, and λ. Table I lists certain characteristics of these orbits.

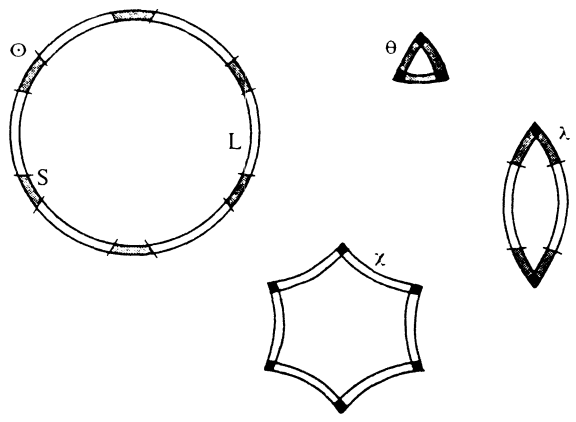

FIG. 3. Basic feasible orbits in the hexagonal magnetic breakthrough lattice of Zn, incorporating the spin degree of freedom. Points denote conduction electron reflection sites at breakthrough vertices, and cuts are breakthrough sites. Conduction electron motion with no spin flip yields the orbit characteristics listed in Table I.

The circular orbit $\odot$ has 12 magnetic breakthrough sites, and it breaks up into six pairs of large regions and six pairs of small ones, designated L and S, respectively, in Fig. 3. Clearly, the other orbits can be constructed from the L and S regions. This partitioning makes it possible to determine the spin contributions $\gamma_{\mathbf{j}}^s$ of all possible orbits in Fig. 3 and to directly calculate the product of factors

$$C_j R_b(j) R_s(j), \tag{16}$$

in accordance with the procedure described above.

There is no difficulty in calculating the resultant amplitudes (16) for the triangular and hexagonal orbits, since there is no spin flip on these orbits. The phase shifts in (13) corresponding to such trajectories with opposite spins thus take different forms: $\gamma_\theta \pm 3\gamma_s$ and $\gamma_\chi \mp 6\gamma_L$. Here $\gamma_j=2\pi F_j/H+\varphi$ is the phase shift acquired by a conduction electron when spin is ignored ($j=\theta,\chi$), and γ_L and γ_s are the spin contributions to the phase shift in large and small regions, respectively. Using these phase shifts and the data from Table I, and summing over the spin, we find

$$C_\theta R_b(\theta) R_s(\theta)=2\tau^3\cos 3\gamma_S, \tag{17}$$

$$C_\chi R_b(\chi) R_s(\chi)=\tau^6\cos 6\gamma_L, \tag{18}$$

for triangular and hexagonal orbits, respectively.

To determine the resultant amplitude consisting of the contributions in (16) for a lune-shaped λ orbit, we need to take account of the spin direction in each region (Fig. 3). In this case there are five pairs of orbits which belong to the lune class. For example, the motion of a conduction electron without spin flip corresponds to the pair of phase shifts $\gamma_\lambda \pm 2(\gamma_L+2\gamma_S)$. A phase shift with spin up, $\uparrow$ (the $+$), is acquired as a conduction electron moves without spin flip through outer regions. A phase shift with spin down, $\downarrow$, is acquired in internal regions. For this pair, expression (16) becomes $3(\rho/\beta)^4\tau^2\cos 2(\gamma_L+2\gamma_S)$.

Incorporating other orbits of this type, and incorporating spin–orbit interaction ($\alpha\neq 0$) and the spin contribu-

TABLE I. Orbit Characters (Fig. 3).

Type of orbit	$\frac{m_j}{m_0}$	Weighting factor C_j	Number of magnetic breakthroughs $n_{1j}+n_{3j}$	Number of reflections n_{2j}	Frequency of de Haas-van Alphen effect F_j (MHz)
1) $\odot$	1	1[a]	12	0	831.26 [14]
2) θ	0.0075 [14]	2	0	3	0.0158 [15]
3) λ	0.337 [1]	3[a]	4	2	47.179 [16]
4) χ	0.986 [1]	1	0	6	543.31 [16]

The weighting factor is only given for one orbit ($n_{3j}=0$).

tions to the phase shift, we find the following result for the resultant magnetic breakthrough amplitude in (13):

$$\sum_{\lambda} C_\lambda R_b(\lambda)R_s(\lambda)=3(\rho/\beta)^4\tau^2\{\cos 2(\gamma_L+2\gamma_S)+4\alpha^2[\cos(\gamma_L+2\gamma_S)\times\cos(2\gamma_S-\gamma_L)-1]+\alpha^4\times\cos 2(2\gamma_S-\gamma_L)\}. \quad (19)$$

For circular orbit $\odot$, with spin flip at each of 12 magnetic breakthrough sites (Fig. 3), we find that 25 pairs of orbits corresponding to the spin directions in the large and small regions arise. Taking account of the symmetry of these orbits, we find 57 products of the type in (16) with different values of $C_\odot$, with even powers of the numbers $n_{1\odot}$ and $n_{3\odot}$, and with combinations of the phase shifts γ_S and γ_L.

As an example, we show how to derive some of these products. In the motion of a conduction electron without spin flip along circular orbit $\odot$ (Fig. 3), for example, the phase shifts in (13) corresponding to trajectories with opposite spins are $\gamma_\odot \pm \pi g_0^S = \gamma_\odot \pm 6(\gamma_L+\gamma_S)$, where g_0^S is the spin-splitting parameter of a circular orbit. Corresponding to the pair of phase shifts $\gamma_\odot \pm (6\gamma_S-2\gamma_L)$ is a single pair of orbits, which differ in spin direction in a symmetric way. The sign in the phase shift in front of $\gamma_L(\gamma_S)$ determines the spin direction in a large region L (in a small region S). Clearly, the replacement $\uparrow \rightarrow \downarrow$ sends one orbit into the other. In this case we have $n_{3\odot}=8$. Taking into account the number of possible orbits in which a conduction electron would acquire such a phase shift, and taking an average over the spin, we find $15(\rho/\beta)^4(\alpha\rho/\beta)^8 \times \cos(2\gamma_S-6\gamma_L)$.

Corresponding to the other pair of phase shifts $\gamma_\odot \pm 4(\gamma_S+\gamma_L)$ are two pairs of orbits with different numbers of magnetic breakthroughs with spin flip. In this case the directions of the spins in one small region S and in one large one L are opposite the spin direction in the other regions. Taking into account all possible orbits and the order in which the conduction electron passes through all the magnetic breakthrough sites, and taking an average over the spin, we find

$$-12(\rho/\beta)^{10}(\alpha\rho/\beta)^2\cos 4(\gamma_S+\gamma_L)$$

and

$$24(\rho/\beta)^2(\alpha\rho/\beta)^{10}\cos 4(\gamma_S+\gamma_L),$$

respectively, for these pairs of orbits.

In a similar way, we find the contributions from the other orbits. Here is the final expression for the resultant magnetic breakthrough amplitude of a circular orbit, which appears in (13) after an average is taken over the spin:

$$\sum_{\odot} C_\odot R_b(\odot)R_s(\odot)=(\rho/\beta)^{12}[\cos(6\gamma_+)+\alpha^2\Sigma(1)+\alpha^4\Sigma(2)+\alpha^6\Sigma(3)+\alpha^8\Sigma(4)+\alpha^{10}\Sigma(5)+\alpha^{12}\cos(6\gamma_-)]. \quad (20)$$

For simplicity we have introduced the following notation here:

$$\gamma_+=\gamma_S+\gamma_L, \quad \gamma_-=\gamma_S-\gamma_L,$$

$$\Sigma(1)=12\{\cos(\gamma_-)[\cos(5\gamma_+)+\cos(3\gamma_+)+\cos(\gamma_+)]-[\cos(4\gamma_+)+\cos(2\gamma_+)+1]\},$$

$$\Sigma(2)=\cos(4\gamma_+)[30\cos(2\gamma_-)+24]-48\cos(\gamma_-)\times[2\cos(3\gamma_+)+3\cos(\gamma_+)]+24\cos(2\gamma_+)\times[2\cos(2\gamma_-)+3]+27\cos(2\gamma_-)+96,$$

$$\Sigma(3)=18\cos(3\gamma_+)[\cos(3\gamma_-)+4\cos(\gamma_-)]+18\cos(3\gamma_-)[\cos(3\gamma_+)+4\cos(\gamma_+)]-36\cos(2\gamma_+)[2\cos(2\gamma_-)+3]-36\cos(2\gamma_-)[2\cos(2\gamma_+)+3]+288\cos(\gamma_+)\cos(\gamma_-)+4\cos(3\gamma_+)\cos(3\gamma_-)-184.$$

The replacements $\gamma_+ \rightarrow \gamma_-$, $\gamma_- \rightarrow \gamma_+$ lead to $\Sigma(2) \rightarrow \Sigma(4)$ and $\Sigma(1) \rightarrow \Sigma(5)$.

To determine the spin increments γ_L and γ_S, it is natural to assume that the cyclotron mass $m_\odot$ and the g-factor $g_\odot$ of circular orbit $\odot$ are equal to the cyclotron mass m_0

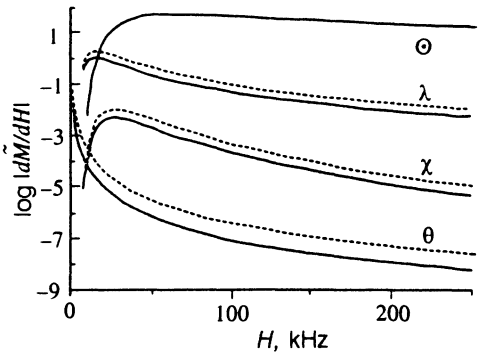

FIG. 4. Field dependence of $\lg|dM/dH|$ for Zn at 1 K; basic orbits in the presence and absence (dashed curves) of spin degrees of freedom. These plots were constructed with no account taken of the Dingle factor. The parameters corresponing to these curves appear in Table I.

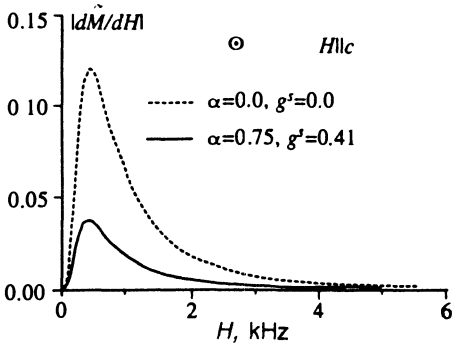

FIG. 6. Field dependence of $|d\tilde{M}/dH|$ for Zn at 1 K; triangular orbit in the presence and absence (dashed curves) of spin degrees of freedom. Parameter values used to construct this curve as in Fig. 4.

and the g-factor $g_0=2$ of a free electron, since this orbit corresponds to a cross section of the Fermi sphere in the model of nearly free electrons. The spin-splitting parameter g_0^s for a circular orbit is then equal to one; i.e., we have $6(\gamma_L+\gamma_S)=\pi$. In a previous study[8] of galvanomagnetic properties of *Zn* we obtained the parameter of the spin splitting at a needle, g^s, which turned out to be 0.41. Assuming that the spin contribution $3\gamma_S$ in (17) of a triangular orbit is equal to πg^s, we find

$$\gamma_S=\pi g^s/3, \quad \gamma_L=\pi(1-2g^s)/6. \tag{21}$$

Substituting (21) into (17)–(20), and using the values of the cyclotron masses and de Haas–van Alphen frequencies from Table I, along with the parameter values $H_0=3.0$ kG and $\alpha=0.75$, found in Ref. 8, we find the resultant oscillation amplitudes $d\tilde{M}_j/dH$ for each orbit. Figures 4–6 show the calculated behavior of the amplitudes $|dM_j/dH|$ as a function of the field for the four orbits which we considered. To bring this illustration closer to the actual situation, we have incorporated a thermal factor R_T [see (12)], in which we have set $T=1$ K.

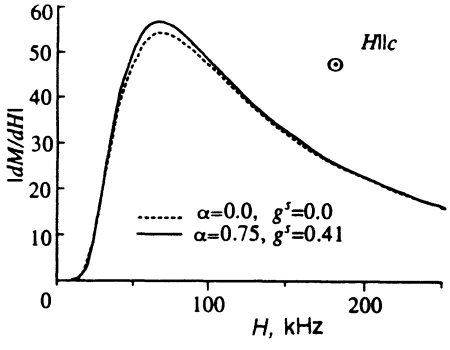

FIG. 5. Field dependence of $|dM/dH|$ for Zn at 1 K; circular orbit in the presence and absence (dashed curves) of spin degrees of freedom. Parameter values used to construct this curve as in Fig. 4.

As in the theory for magnetic breakdown without spin flip which has been derived for Mg (Refs. 1 and 5), the amplitude of the oscillations from χ and θ orbits naturally decreases as the field increases, while the oscillations from the other orbits ($\odot$ and λ) become predominant to the extent that magnetic breakthrough plays an increasingly important role. Incorporating the spin–orbit interaction and the spin degrees of freedom of conduction electrons leads to a significant decrease in the amplitude of the de Haas–van Alphen oscillations from all orbits except the circular one. The reason is that the orbit $\odot$ passes through a large number of magnetic breakthrough sites, and at each such site there may be a spin flip of a conduction electron. There will be an increase in the number of possible paths, each of which is determined by its own magnetic breakthrough amplitude. There is thus an increase in the probability for finding conduction electrons with opposite spin directions on this orbit. This probability depends in a complicated way [see (20)] on the spin–orbit parameter α and on the g-factors of the various regions.

The behavior of the oscillations from a θ orbit passing through a needle in Zn served as one of the early pieces of evidence for the existence of magnetic breakthrough.[1] When the spin is taken into account, the maximum of the amplitude (Fig. 6) decreases by a factor of more than 2. The addition of a factor $R_s=\cos(\pi g^s)$ in (13) does indeed lead to a good explanation of the strong dependence of the amplitude of the de Haas–van Alphen oscillations on the value of the g-factor at the needles as observed experimentally.[10] In addition, the spin properties of conduction electrons substantially alter the nature of these oscillations, as follows from the complicated way in which the magnetic breakthrough amplitude depends on the spin–orbit parameter α and the g-factor.

4. DE HAAS–VAN ALPHEN OSCILLATIONS IN THE COURSE OF MAGNETIC BREAKDOWN; SPIN-INDUCED SPLITTING OF LANDAU LEVELS AT NEEDLES IN Zn

It is interesting to substitute the characteristics found for the magnetic breakthrough of a system (in particular, the parameters of the needles) through a comparison of theory and experiment on the galvanomagnetic properties

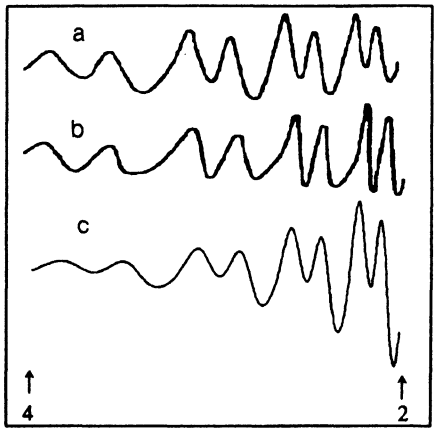

FIG. 7. Oscillations in $d^2\tilde{M}/dH^2$ at "needles" ub Zn;H parallel to hexagonal axis and $T=12$ K. Parameter values corresponding to curve (c) given in text. Experimental (a) and theoretical (b) curves reproduced from Ref. 10.

of Zn (Ref. 8) into the theoretical expressions for the de Haas–van Alphen effect and to compare them with the experimental results available. We know of only one study in which spin splitting of energy levels in a magnetic field under magnetic breakthrough conditions has been observed in de Haas–van Alphen oscillations involving needles in Zn at a temperature $T=1.2$ K (Ref. 10). This comparison of theory and experiment is basically of an illustrative nature, since in this case of a triangular orbit, spin–orbit interaction does not play the substantial role that it would play in the case of lune-shaped or circular orbits. The reason is that there is no spin flip of a conduction electron as it moves along this orbit. Figure 7a is a plot of the experimental behavior of the second derivative of the magnetization with respect to the magnetic field.

The generalization of the theory for the de Haas–van Alphen effect under magnetic breakthrough conditions to the case in which there is spin–orbit interaction—i.e., the content of the preceding sections of this paper—makes it possible to derive an expression for $d^2\tilde{M}(H,T)/dH^2$ for a triangular orbit of Zn (Fig. 3) in a more systematic way than in Ref. 10. Taking yet another derivative of expression (13) with respect to the field, and incorporating the Dingle factor, we easily find an expression for the corresponding quantity:

$$\frac{d^2\tilde{M}(T,H)}{dH^2}=\left(\frac{e}{c\hbar}\right)^{3/2}\left(\frac{m_0}{m}\right)^{1/2}\frac{4\pi k_B T F^3}{H^{9/2}}\sum_{r=1}^{\infty}\times r^{3/2}\frac{\exp(-\alpha r x/H)}{\mathrm{sh}(\alpha r T/H)}\times C_\theta \tau^{3r}\cos(\pi r g^s)\sin\left[r\left(\frac{2\pi F}{H}+3\Lambda-2\pi\gamma\right)-\frac{\pi}{4}\right], \quad (22)$$

where x is the Dingle temperature, which is determined by the mean scattering time of a conduction electron, 3Λ is the sum of the phase shifts from the three magnetic breakdown sites [see (5c)], α is given by (14), and we have $g^s=0.41$ (Ref. 8). The argument of the gamma function in (5c) can be expressed in terms of simple functions[17] (Im $y=0$):

$$\arg\Gamma(iy)=-Cy-\frac{\pi}{2}+\sum_{n=1}^{\infty}[y/n-\mathrm{arctg}(y/n)],$$

where C is the Euler constant. We restrict the summation over r in (22) to ten terms ($r=1$–10), which dominate the sum. The values of the other parameters in (22) correspond to the values of Ref. 8, which were used in plotting Fig. 6 ($H_0=3$ kG, $\alpha=0.75$, $F=0.0158$ MG). A theoretical curve found for $T=1.2$ K, for a Dingle temperature[10] $x=1.5$, for[6] $g^2=0.41$, and for $\gamma=0.21$ is shown in Fig. 7c. It is clear from Figs. 7a and 7c that the theoretical and experimental curves agree in terms of their behavior, the frequency dependence, and the presence of obvious split peaks. We regard all this as demonstrating that the results are in qualitative agreement. We thus have more confidence in the estimates of Ref. 8.

Since there is no spin flip of a conduction electron as it moves along a triangular orbit, the curve found here (Fig. 7c) does not differ in any substantial way from the theoretical curve found in Ref. 10 (Fig. 7b). There is an important distinction between the different approaches: our results are derived in a systematic way from magnetic breakthrough theory,[6] which incorporates the spin degrees of freedom (in particular, γ_s and α) at a microscopic level. In Ref. 10, in contrast, parameters describing the spin-induced splitting of peaks were introduced in a phenomenological way. They were found by fitting a theoretical curve to experimental data. In addition, in order to improve the agreement with experiment, it was found necessary in Ref. 10 to use a characteristic breakdown field $H_0=5$ kG in the calculations. That field differs from the value $H_0\sim 3$ kG found from other experiments.[1,3,8] The present paper, in contrast, uses parameters (the de Haas–van Alphen frequency, H_0, α, and—most importantly—the value of a needle conduction-electron g-factor) found independently in a study of galvanomagnetic properties of zinc. These values agree well with other values which have been reported.

We also note that Λ is present in a phase in (22). This quantity is a complicated function of H [see (5c)] and of the quantity H_0, renormalized for the spin–orbit interaction. The magnetic breakthrough phase shift Λ follows from the solution of the quantum Schrödinger equation at magnetic breakthrough sites[4,6] and is a strong function of the ratio H_0/H. In the case under discussion here, 3Λ ranges from –0.49 at $H=1.67$ kG to –1.02 at $H=4$ kG for a value $\alpha=0.75$ of the spin–orbit parameter. Only a constant phase shift of $2\pi\gamma$ was taken into account in Ref. 10, and the parameter γ had to take on one of the two values 0.32 or 0.82 for a description of the position of the spin-split peaks. Incorporating this difference in phase leads in our case (Fig. 7c) to the result that the dips between the

peaks corresponding to different spin states are smaller than in the old theory (Fig. 7b). We believe that this result is in agreement with experiment (Fig. 7a).

On the other hand, as in Ref. 10, we are left with a rather large discrepancy between experiment and theory regarding the position of the peak in the oscillation amplitude, which is shifted toward lower fields on the theoretical curve: $H_{\max}^{\text{theor}}=0.75$ kG $< H_{\max}^{\text{exp}} \simeq 2.2$ kG. Unfortunately, we are unable to compare the amplitude characteristics more precisely, since the experimental results are expressed in arbitrary units, and we do not know the step size of the changes in the field H during the measurements. The theoretical curve in Fig. 7c is plotted for a field step size of 2.5 G. At this step size, it is possible to accurately determine the amplitude in low fields. As the step size in the field increases in the tabulation of (22), a false pattern emerges: the oscillation amplitude decreases in low fields. The reason for this decrease is that function (22) has some extremely sharp peaks at H below 1.5 kG, and the procedure by which this function was tabulated, with a large step size, simply skips over local extrema in this field range. This circumstance may partially explain the discrepancy between the experimental and theoretical results.

Another possible reason for the deviations of our theory (for the de Haas–van Alphen effect under magnetic breakdown conditions, with spin–orbit interaction) from experiment is that we have ignored certain effects, such as magnetic interactions, many-body interactions, and nonuniformity of the sample.

We wish to thank M. I. Kaganov for some stimulating discussions and valuable comments, and also B. I. Kochelaev for support. We also thank the American Physical Society (the Sloan Foundation) for partial support of this study.

[1)]We will also use the common term "magnetic breakthrough network."[1,3,5]

[2)]The sum of γ and Λ_j constitutes the quantum correction to the Lifshitz–Onsager 1/2 formula, which is ordinarily used.[2,10]

[3)]The same can be said of closed loops which belong to a common band and which may be part of a j-orbit.

[4)]Here we are considering only the longitudinal component of the susceptibility $d\widetilde{M}/dH=-(\partial^2\widetilde{\Omega}/\partial H^2)_\mu$, where μ is the chemical potential.

[5)]This is the usual procedure in the derivation of an expression for $\widetilde{\Omega}$, since $g\mu_B H \ll \mu$, where g and μ_B are the g-factor and the Bohr magneton, respectively.

[6)]This value of the spin contribution corresponds to a value ~ 109 for the effective g-factor of the conduction electrons of the needles.[8]

[1] D. Schoenberg, *Magnetic Oscillations in Metals* Cambridge Univ. Press, New York (1984).
[2] I. M. Lifshits, M. Ya. Azbel', and M. I. Kaganov, *Electron Theory of Metals,* Nauka, Moscow (1971).
[3] R. W. Stark and L. M. Falicov, Progr. Low Temp. Phys. **5**, 235 (1967).
[4] M. I. Kaganov and A. A. Slutskin, *Conduction Electrons* [in Russian], Nauka, Moscow (1985).
[5] L. M. Falicov and H. Stachowiak, Phys. Rev. **147**, 505 (1966).
[6] Yu. N. Proshin, Zh. Eksp. Teor. Fiz. **93**, 1356 (1987) [Sov. Phys. JETP **66**, 770 {1987)].
[7] Yu. N. Proshin and T. L. Noskova, Abstracts, Twenty-Ninth Conference on Low-Temperature Physics [in Russian], Kazan' (1992), Part 2, p. 353.
[8] Yu. N. Proshin and N. Kh. Useinov, Zh. Eksp. Teor. Fiz. **100**, 1088 (1991) [Sov. Phys. JETP **73**, 602 (1991)].
[9] R. W. Stark, Phys. Rev. **A135**, 1698 (1964).
[10] W. J. O'Sullivan and J. E. Schirber, Phys. Rev. **162**, 519 (1967).
[11] J. Jafet, Solid State Phys. **14**, 1 (1963).
[12] A. A. Slutskin, Zh. Eksp. Teor. Fiz. **58**, 1098 (1970) [Sov. Phys. JETP **31**, 589 (1970)].
[13] A. A. Slutskin, *Conduction Electron Dynamics and Kinematic Phenomena in Metals Under Magnetic Breakthrough Conditions, Dissertation,* Institute of Low-Temperature Phyhsics and Technology (FTINT), Khar'kov, Ukrainian Academy of Sciences (1980).
[14] W. A. Harrison, Phys. Rev. **126**, 497 (1962).
[15] A. S. Joseph and W. L. Gordon, Phys. Rev. **126**, 489 (1962).
[16] A. C. Thorsten, L. E. Valby, and A. S. Joseph, *Proceedings of the Ninth International Conference on Low-Temperature Physics,* New York (1965).
[17] M. Abramowitz and I. A. Stegun (eds), *Handbook of Mathematical Functions,* Dover, New York (1965).

Translated by D. Parsons